

Pyrolytic carbon from biomass precursors as anode materials for lithium batteries

A. Manuel Stephan^{a,b}, T. Prem Kumar^b, R. Ramesh^b, Sabu Thomas^c,
Soo Kyung Jeong^a, Kee Suk Nahm^{a,*}

^a School of Chemical Engineering and Technology, Chonbuk National University, Chonju 561-756, South Korea

^b Central Electrochemical Research Institute, Karaikudi 630006, India

^c School of Chemical Sciences, Mahatma Gandhi University, Kottayam 686560, India

Received 20 February 2006; received in revised form 28 April 2006; accepted 17 May 2006

Abstract

Disordered carbonaceous materials were synthesized by the pyrolysis of banana fibers treated with pore-forming substances such as ZnCl_2 and KOH. X-ray diffraction studies indicated a carbon structure with a large number of disorganized single layer carbon sheets. Addition of porogenic agent led to remarkable changes in the structure and morphology of the carbonaceous products. The product obtained with ZnCl_2 treatment gave first-cycle lithium insertion and de-insertion capacities of 3325 and 400 mAh g^{-1} , respectively. Lower capacities only could be realized in the subsequent cycles, although the coulombic efficiency increased upon cycling, which in the 10th cycle was 95%.
© 2006 Elsevier B.V. All rights reserved.

Keywords: Carbon anode; Pyrolytic carbon; Porogen; Banana fiber; Lithium-ion battery

1. Introduction

For more than a decade now lithium batteries have been available electronic gadgets such as laptop computers, digital cameras and portable memory devices. The ambit of their application is being gradually extended to the transport sector where they are envisaged as the sole power source and in hybrid modes with fuel cells and supercapacitors [1,2]. Therefore, high-rate capability and relatively cheap electro-active materials are required for the development of high-power lithium-ion batteries. A key element in lithium-ion battery technology is the lithiated carbon anode. Graphitic carbons that are the mainstay of anodes in today's lithium-ion technology have a theoretical specific capacity of 372 mAh g^{-1} , which is about a tenth of that of metallic lithium. Much attention has, therefore, been devoted to anode materials with higher specific capacities. Among these are low-crystalline carbons, which can accommodate much higher amounts of lithium than graphite. Disordered carbons have several attractive features [3–5]: (i) a higher lithium intake than the theoretical limit of 372 mAh g^{-1} for perfectly graphitic materi-

als; (ii) amenability to tailoring by varying the nature of their organic precursors and temperature protocols; (iii) good cycling properties.

Disordered carbons prepared by pyrolysis of organic precursors contain a predominantly planar hexagonal network of carbon atoms, but lack extended crystallographic ordering. Pyrolytically prepared carbons have also been shown to retain up to 30 at.% of residual hydrogen. The high lithium capacities of pyrolytic carbons are associated with both disorder [5–7] and hydrogen content [3,5,8]. Several such carbons have been obtained by pyrolysis of biomass precursors such as walnut and almond shells [9], peanut shells [10], lignin, cotton and wool [11], rice husk [12], starch and oak [9] and sugar [9,13–17]. In this paper, we present our results on the lithium-insertion properties of pyrolytic carbons obtained from banana fibers treated with ZnCl_2 or KOH as a porogen.

2. Experimental

High-quality banana fibers were obtained from fields in Kerala, India. Sheets of the herbaceous stems were dried in the sun and fibers were mechanically drawn from them. The fibers were then soaked in water, washed and dried. The brownish white dry

* Corresponding author. Tel.: +82 63 270 2311; fax: +82 63 270 2306.
E-mail address: nahmks@chonbuk.ac.kr (K.S. Nahm).

fibers were then treated with concentrated solutions of ZnCl_2 or KOH for 5 days at 110°C at a fiber:porogen ratio of 1:5 by weight, and dried. Pyrolysis was carried out by heating under flowing nitrogen at 800°C at a heating ramp of $10^\circ\text{C min}^{-1}$ for a hold period of 1 h. Pyrolytic carbons were also obtained without treatment with the porogen, in which case, the fibers simply heat-treated under the above conditions.

Elemental analysis was done by a Perkin-Elmer CHN 2000 elemental analyzer. Powder X-ray diffraction patterns were recorded between 10° and 80° on a Jeol X-ray diffractometer, model (D/Max 2500) fitted with a nickel-filtered $\text{Cu K}\alpha$ radiation source. The morphologies of the pyrolytic carbons were examined by a (FESEM S-4700, Hitach) scanning electron microscope. BET surface area measurements were carried out on a (Micromeritics ASAP 2010) surface area analyzer. FT-IR spectra were recorded on a (Perkin-Elmer Paragon 500 FT-IR) spectrophotometer. Carbon electrodes for electrochemical lithium-insertion studies were prepared by blade-coating a slurry of 85 wt.% of the pyrolytic carbon, 12 wt.% of poly(vinylidene fluoride) and 2 wt.% MCMB dispersed in *N*-methyl-2-pyrrolidone on a copper foil, followed by drying at 110°C in an air oven, roller-pressing the dried sheets, and punching out circular sheets. The carbon electrodes were coupled with lithium (Foote Minerals) with an electrolyte of 1 M LiPF_6 in a 1:1 (v/v) mixture of EC-DEC in swage-lock cells in an argon-filled glove box (M Braun, Germany). Galvanostatic charge–discharge profiles were made between 2.500 and 0.020 V on a computer-controlled battery testing unit (Maccor, 4000, USA).

3. Results and discussion

3.1. H/C ratio and surface area

Table 1 gives values of H/C ratio, average pore diameter and BET surface area of the pyrolytic carbons. It can be seen from the Table 1 that the H/C ratio of the porogen-treated fiber carbons is lesser than that of the untreated one. It is possible that the heat generated during the decomposition of the porogen or any chemical reaction of the products of decomposition of the porogen with the fibers might have altered the chemical composition of the carbonaceous products. Porosity in carbonaceous materials can be generated by use of several chemical activation agents such as Na_2CO_3 , K_2CO_3 , NaOH, KOH, H_3PO_4 , AlCl_3 , MgCl_2 , LiCl and ZnCl_2 are employed. In this work we have used KOH and ZnCl_2 for activation. Despite the large volume of literature on chemical activation, the mechanisms of the processes are yet to be fully elucidated [18–24]. It is, however, generally believed

Table 1
The atomic hydrogen to carbon ratio (H/C), average pore diameter and BET surface area of the pyrolytic carbons

Sample	H/C ratio	Pore diameter (Å)	BET surface area (m^2g^{-1})
Without porogen	30	19	36
ZnCl_2 treated	26	57	1285
KOH treated	24	24	751

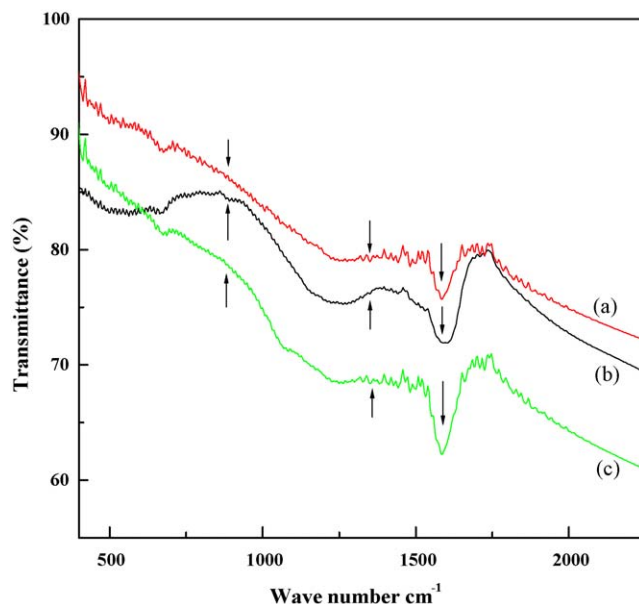


Fig. 1. FT-IR spectra of pyrolytic carbons derived from: (a) untreated fiber; (b) fiber treated with ZnCl_2 ; (c) fiber treated with KOH.

that ZnCl_2 acts as a dehydrating agent [19,25,26] and, upon carbonization, leads to charring and aromatization of the carbon skeleton and creation of pore structure [19,26]. ZnCl_2 at high concentrations is known to give Bronsted acidity to the activation solution, and to dissolve cellulosic constituents of biomass [24]. In the case of KOH, the oxygen in the alkali removes the cross-linking and stabilizes the carbon atoms in crystallites [27]. Metallic potassium obtained at the pyrolysis temperature may intercalate and force apart the lamellae of the crystallites [27]. Removal of metallic potassium by, say, washing creates micro-porosity in the new structure [27,28,29].

Furthermore, the surface area and pore diameter of the products are greatly varied due to the action of the porogens. For example, the pore diameter increased from 19 Å for the untreated fiber carbon to 57 and 24 Å for the products obtained by treatment with ZnCl_2 and KOH, respectively. The attendant increase in the BET surface area was from 37 to 1285 and 751 m^2g^{-1} for the ones after treatment with ZnCl_2 and KOH, respectively. Thus, the pore size has been increased up to three-fold, while the surface area increased 35 times because of the action of the porogens. The microstructural evolutions can significantly influence the electrochemical behavior of the carbons.

3.2. FT-IR analysis

Fig. 1 shows the FT-IR spectra of the carbons obtained with and without porogen treatment. The characteristic peak around 1650 cm^{-1} is ascribed to $\nu_{\text{C}=\text{O}}$ (asymmetric stretching), the peak around 1400 cm^{-1} to δ_{CH_2} , and those around 1300 and $1000\text{--}1200\text{ cm}^{-1}$ to $\nu_{\text{C}=\text{O}}$ (symmetric stretching) and $\nu_{\text{C}-\text{O}}$, respectively. The oxygen in the carbons are present in functional groups such as carboxyls, carboxyl anhydrides, phenols, carbonyls, lactones, quinines, quinine-like structures, etc. [18]. These functional groups appear at edge carbon atoms, and are

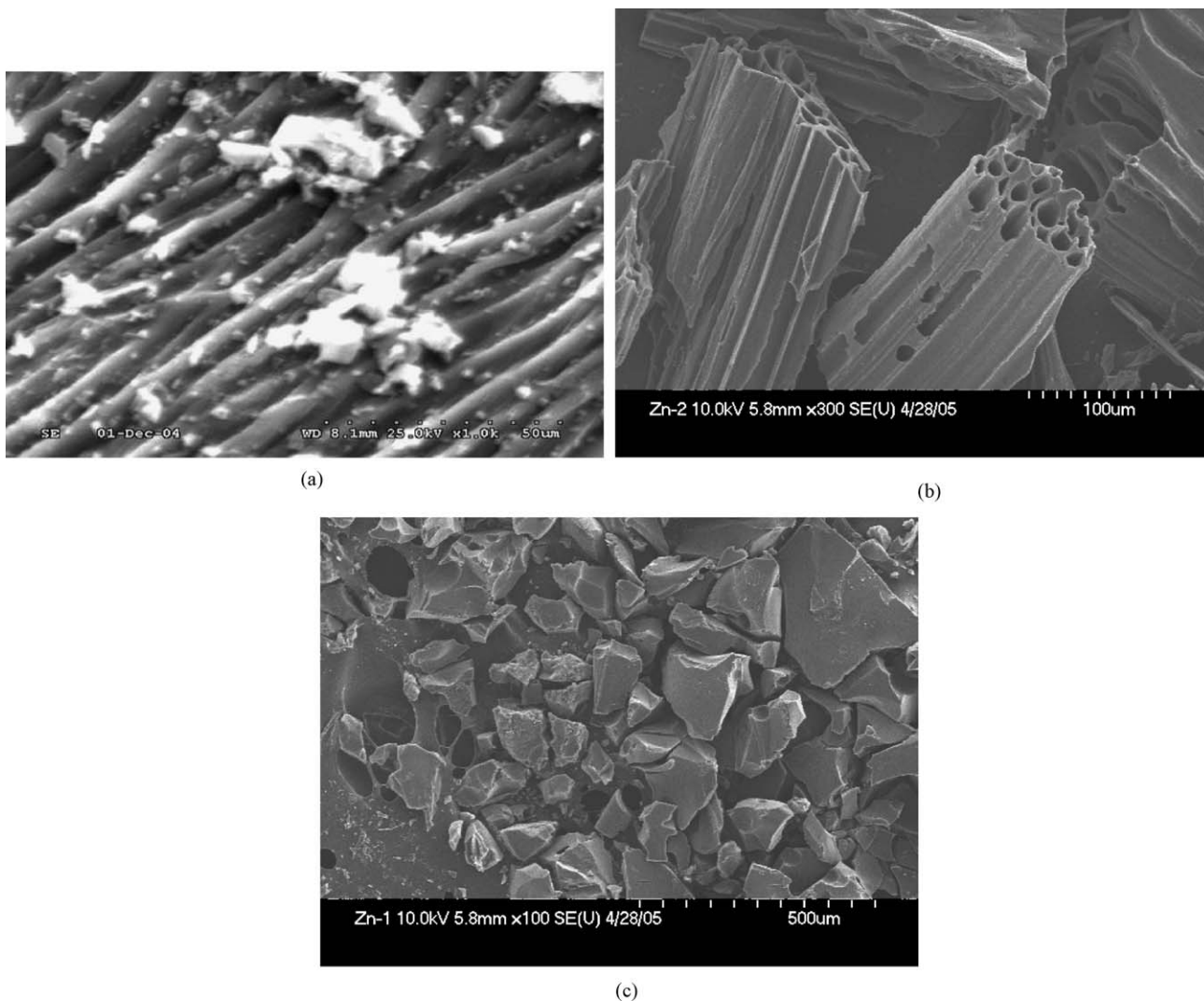


Fig. 2. SEM micrographs of pyrolytic carbons derived from: (a) untreated fiber; (b) fiber treated with ZnCl₂; (c) fiber treated with KOH.

formed during the pyrolysis process. Similar observations have been reported by Naoi et al. [30].

3.3. SEM examination

Fig. 2 depicts the SEM micrographs of banana carbons obtained with and without porogen treatment. The porogen-free carbon shows a tube-like structure (Fig. 2(a)). On the other hand, the carbon upon treatment of the fiber with ZnCl₂ seems to have large aligned fibrous stacks, parts of which seem to have been blown off by the emanating gases. More interestingly, the KOH-treated fiber carbons have a loose, disjointed structure with particularly no shape.

3.4. XRD analysis

Fig. 3(a)–(c) shows the XRD patterns of the carbon samples. They are typical of disordered carbons although the characteristic (002) and (100) peaks of graphite are still discernible. The (100) reflections around 43° honeycomb structures formed

by sp² hybridized carbons, while the broad (002) reflections between 20° and 30° indicate small domains of coherent and parallel stacking of the grapheme sheets. According to Liu et al. [31] the empirical parameter, *R*, defined as the ratio of the height of the (002) Bragg reflection to that of background and is a measure of the quantity of single layered carbon sheets in disordered carbons prepared by low-temperature pyrolysis. Low values of the *R* factor for the samples (untreated: 2.31; ZnCl₂-treated: 2.27; KOH-treated: 2.02) suggest large concentrations of non-parallel single layers of carbon. The increase in the *R* value upon treatment with the porogens suggests a breakdown of aligned structural domains in the carbon matrix.

3.5. Galvanostatic charge–discharge cycling

The carbons obtained by pyrolysis of both porogen-treated and untreated fibers were subjected to charge–discharge cycling between 2.500 and 0.020 V at a 0.1 C rate (with respect to the theoretical value of 372 mAh g^{−1} for graphite). The first cycle insertion and deinsertion capacities for the carbons from the

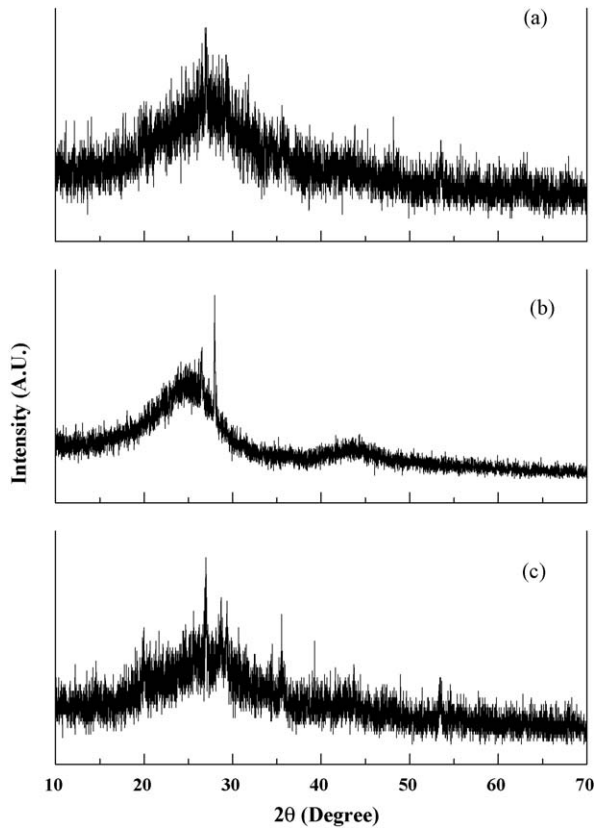


Fig. 3. XRD patterns of pyrolytic carbons derived from: (a) untreated fiber; (b) fiber treated with ZnCl₂; (c) fiber treated with KOH.

untreated fibers were 625 and 310 mAh g⁻¹, respectively. In other words, the loss in capacity in the first cycle is 50% for this material.

Fig. 4(a)–(c) shows the charge–discharge curves of carbons derived from untreated, ZnCl₂, KOH treated banana carbons.

Also Table 2 and Fig. 5 show that the first-cycle insertion capacities for the carbons from the porogen-treated fibers are 3123 and 921 mAh g⁻¹ for ZnCl₂ and KOH, respectively. However, the first-cycle deinsertion capacities are 401 and 356 mAh g⁻¹, corresponding to coulombic efficiencies of only 12.8 and 38.7%. The large loss in capacity means that a significant part of the lithium is unavailable for reversible

Table 2
The insertion and de-insertion capacities of KOH and ZnCl₂ treated banana carbon

Cycle no.	IC ZnCl ₂	DC	IC KOH	DC KOH
1	3123	401	921	356
2	419	243	440	306
3	261	184	380	286
4	211	178	345	298
5	173	146	253	285
6	142	147	250	248
7	138	154	242	238
8	134	145	238	240
9	124	138	226	228
10	123	129	217	204

IC: insertion capacity (mAh g⁻¹); DC: deinsertion capacity (mAh g⁻¹).

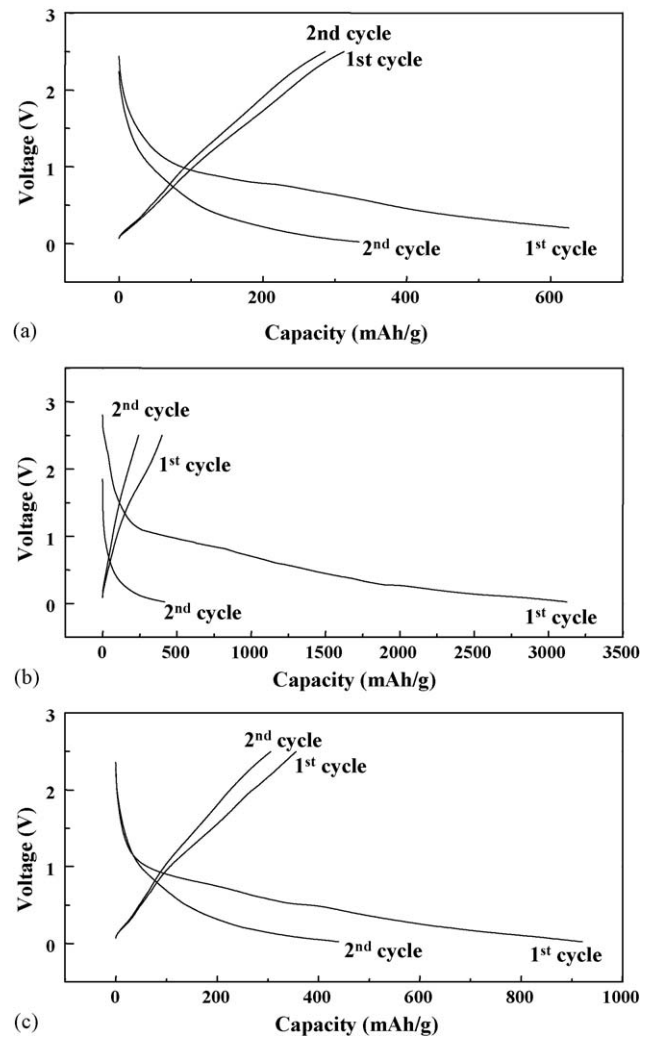


Fig. 4. Charge–discharge curves of carbons derived from: (a) untreated; (b) ZnCl₂; (c) KOH treated carbon.

reactions, rendering a significant part of the active material deadweight. Moreover, since the primary source of lithium is the lithiated cathode, low anode efficiency means inability to

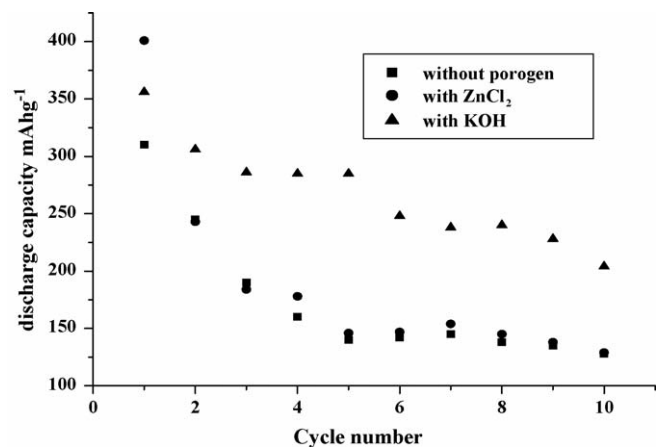


Fig. 5. Cycling behavior of pyrolytic carbons derived from banana fibers. (■) untreated; (●) treated with ZnCl₂; (▲) treated with KOH.

completely re-lithiate the cathode. The coulombic efficiencies in the subsequent cycles gradually increase and stabilize to nearly 100%. In a couple of cases, the deintercalation capacities are slightly larger than the amount of lithium inserted in the previous charging. It is believed that some of the lithium inserted goes into deep sites in the carbon matrix, which renders them irretrievable. However, the larger deinsertion capacity suggests that there is a constant realignment of the single layer carbon layers, during which some of the inserted lithium get “exposed” and become available for the electrochemical cycling.

The high first-cycle insertion and irreversible capacities are attributable to: (i) high H/C ratios (Table 1) [21,22]; (ii) presence of a large number of nanopores [23–25]; (iii) large surface areas with reactive functional groups that provide ample sites for passivation. Hydrogen-containing carbons exhibit large capacities proportional to the hydrogen content; they also exhibit large hysteresis in their charge-discharge profiles [21,22]. Hydrogen in the carbons is believed to “saturate” the dangling bonds on the edge carbon atoms, generating polyaromatic hydrocarbons [8]. Based on their *ab initio* calculations, Papanek et al. [8] have shown that the energies required for lithium intercalation and for lithium to bind to these hydrogen-saturated sites were quite close, which means that both these processes occur at similar potentials. Dahn et al. [31,32,33] attribute the large hysteresis in hydrogen-containing carbons to (H–C)–Li bridging, by which a two-coordinated edge carbon would transform from the sp^2 to the sp^3 hybridized form.

As we have seen earlier, these disordered carbons have a predominance of unorganized single carbon layers, which can provide sites for accommodating lithium during charge. According to Dahn’s “falling cards” model [26], at low pyrolytic temperatures at which these carbons are formed, the thermal energy insufficient to rotate graphene sheets into parallel alignment and into stacks. Thus, low-temperature carbons have a large number of non-parallel, unorganized single layers of hexagonal carbons, a fact reflected in the low values of the R parameter. The presence of such uncorrelated graphene fragments and sheets plays an important role in the amount of lithium a disordered carbon can accommodate [5]. According to Mabuchi et al. [34], the “excess” capacity is due to lithium occupying sites inside nanopores that are present between layers in disordered carbons from which it is often difficult to retrieve the inserted lithium. Such pores facilitate insertion of large amounts of lithium, part of which is lost due to extensive passivation [35,36]. The products of passivation gradually clog the openings of the pores and cavities, rendering the lithium trapped in the pores unavailable for further cycling. The large first-cycle insertion capacity realized with the carbon produced from the $ZnCl_2$ -treated fiber is commensurate with the large surface area of the carbon [37,38].

However, the large surface area can also expose a large surface for passivation. Additionally, the large pores that are generated in this carbon do not serve as lithium-accommodating cavities. Instead, they allow access to electrolyte, which can in turn passivate the pore surface, raising the irreversible capacity. Unlike the SEI, clogging of the pores must necessarily involve formation of pores into thick layers, which impede electrolyte

access to the active carbon surface. Thus, the masking of the carbon surface would lead to a lower retrieval of stored lithium in the carbons.

It is thus clear that large pores are pejorative to carbon-based anodes. Such pores facilitate simultaneous interaction of lithium with surface functional groups and plating on the carbon surface followed by passivation upon reaction with the electrolyte. On the other hand, small can be active lithium-accommodating sites.

4. Conclusions

High-surface area disordered carbons prepared by the pyrolysis of banana fibers treated with $ZnCl_2$ and KOH as pore-formers have been shown to accommodate lithium up to 3123 mAh g^{-1} . However, their high first-cycle irreversible capacities of as much as 87.8% is a matter of concern. The large initial and irreversible capacities are explained in terms of high hydrogen content, large surface area, the R parameter and pores. Irretrievability of trapped lithium, surface passivation and clogging of pores and cavities are factors that contribute to large coulombic inefficiencies.

Acknowledgements

This work was supported by the Korea Research Foundation Grant funded by the Korean Government (MOEHRD) (KRF-2005-005-J07501). One of the authors (AMS) gratefully acknowledges Prof. A.K. Shukla, Director, CECRI, Karaikudi, India for granting extraordinary leave.

References

- [1] M. Broussely, J. Power Sources 81–82 (1999) 140–143.
- [2] R. Vissers, M.M. Thackeray, J. Power Sources 81–82 (1999) 902–905.
- [3] T. Zheng, Y. Liu, E.W. Fuller, S. Tseng, U. von Sacken, J.R. Dahn, J. Electrochem. Soc. 142 (1995) 2581–2584.
- [4] S. Yata, H. Kinoshita, M. Komori, N. Ando, T. Kashiwamura, T. Harada, K. Tanaka, T. Yamabe, Synth. Met. 62 (1994) 153–158.
- [5] J.R. Dahn, T. Zheng, Y.H. Liu, J.S. Xue, Science 270 (1995) 590–593.
- [6] K. Sato, M. Noguchi, A. Demachi, N. Oki, M. Endo, Science 264 (1994) 556.
- [7] R. Yazami, M. Deschamps, J. Power Sources 54 (1995) 411–415.
- [8] P. Papanek, M. Radosavljevic, J. Fisher, Chem. Mater. 8 (1996) 1519–1524.
- [9] W. Xing, J.S. Xue, T. Zheng, A. Gibaud, J.R. Dahn, J. Electrochem. Soc. 143 (1996) 3482–3486.
- [10] G.T.K. Fey, D.C. Lee, Y.Y. Lin, T. Prem Kumar, Synth. Met. 139 (2003) 71–80.
- [11] E. Peled, V. Eshkenazi, Y. Rosenberg, J. Power Sources 76 (1998) 153–158.
- [12] G.T.K. Fey, C.L. Chen, J. Power Sources 97/98 (2001) 47–51.
- [13] A. Gibaud, J.S. Xue, J.R. Dahn, Carbon 34 (1996) 499–503.
- [14] W. Xing, R.A. Dunlap, J.R. Dahn, J. Electrochem. Soc. 145 (1998) 62–70.
- [15] G.T.K. Fey, Y.C. Kao, Mater. Chem. Phys. 73 (2002) 37–43.
- [16] G.T.K. Fey, K.L. Chen, Y.C. Chang, Mater. Chem. Phys. 76 (2002) 1–6.
- [17] W. Xing, J.S. Xue, J.R. Dahn, J. Electrochem. Soc. 143 (1996) 3046–3050.
- [18] P. Ehrburger, A. Addoun, F. Addoun, J.B. Donnet, Fuel 65 (1986) 1447.
- [19] F. Caturla, M. Molina-Sabio, F. Rodriguez-Reinoso, Carbon 29 (1991) 999.

- [20] M. Molina-Sabio, F. Rodriguez-Reinoso, F. Caturla, M.J. Selles, Carbon 33 (1995) 1105.
- [21] A. Ahmadvpour, D.D. Do, Carbon 34 (1996) 471.
- [22] Z. Hu, M.P. Srinivasan, Y. Ni, Carbon 39 (2001) 877.
- [23] C. Moreno-Castilla, F. Carrasco-Marin, M.V. Lopez-Ramon, M.A. Alvarez-Merino, Carbon 39 (2001) 1415.
- [24] M. Molina-Sabio, F. Rodriguez-Reinoso, Coll. Surf. A 241 (2004) 15.
- [25] F. Rodriguez-Reinoso, M. Molina-Sabio, Carbon 30 (1992) 1111.
- [26] S. Balei, T. Dogu, H. Yucel, J. Chem. Technol. Biotechnol. 60 (1994) 419.
- [27] H. Marsh, D.S. Yan, T.M. O'Grady, A. Wennerberg, Carbon 22 (1984) 603.
- [28] T. Otowa, R. Tanibata, M. Itoh, Gas Sep. Purif. 7 (1993) 241.
- [29] H.P. Boehm, Carbon 26 (1988) 363–373.
- [30] K. Naoi, N. Ogihara, Y. Igarashi, A. Kamakura, Y. Kusachi, K. Utsugi, J. Electrochem. Soc. 152 (2005) A1047–A1052.
- [31] Y. Liu, J.S. Xue, J.R. Dahn, Carbon 34 (1996) 193–200.
- [32] J.R. Dahn, T. Zheng, Y. Liu, J.S. Xue, Science 264 (1994) 556–560.
- [33] T. Zheng, J.S. Xue, J.R. Dahn, Chem. Mater. 8 (1996) 389–392.
- [34] A. Mabuchi, Tanso 165 (1994) 298–302.
- [35] K. Tokumitsu, A. Mabuchi, H. Fujimoto, T. Kasuh, J. Power Sources 54 (1995) 444–447.
- [36] G. Sandi, R.E. Winans, K.A. Carrado, J. Electrochem. Soc. 143 (1996) L95–L97.
- [37] J.R. Dahn, W. Xing, Y. Gao, Carbon 35 (1997) 825–830.
- [38] H. Fujimoto, A. Mabuchi, K. Tokumitsu, T. Kasuh, J. Power Sources 54 (1995) 440–443.